Two-dimensional MXene incorporated chitosan mixed-matrix membranes for efficient solvent dehydration

Zhi Xu[1], *Guozhen Liu*[2], *Hua Ye*[1], *Wanqin Jin*[2] *and Zhanfeng Cui*[1]*

[1]CRMI Technology Centre, Institute of Biomedical Engineering, Department of Engineering Science, University of Oxford, Oxford, UK.

[2]State Key Laboratory of Materials-Oriented Chemical Engineering, College of Chemical Engineering, Nanjing Tech University, 5 Xinmofan Road, Nanjing 210009, PR China.

*Corresponding author: zhanfeng.cui@eng.ox.ac.uk

Abstract

Pervaporation dehydration is an energy efficient process for purifying organic solvents, whose application depends on the development of highly permeable and selective membranes. In this work, synthesized two-dimensional $Ti_3C_2T_x$ MXene nanosheets were incorporated into chitosan (CS) to fabricate a new MXene/CS mixed-matrix membrane used for solvent dehydration via pervaporation process. The morphology, chemical structure and surface hydrophilicity of the membranes were studied by SEM, AFM, IR, XPS and water contact angle measurement. Three kinds of organic solvents, ethanol, ethyl acetate and dimethyl carbonate were used for evaluating the membrane dehydration performance. The results indicated that incorporation of MXene nanosheets did not increase the surface sorption, whereas the assembled MXene laminates with interlayer channels greatly enhanced the permeation of water molecular through the membrane. Thus, flux and separation factor of CS membrane were simultaneously improved by introducing the MXene nanosheets. Specifically, the optimized 3 wt% MXene/CS MMM exhibited total flux of ~1.4-1.5 kg/(m^2 h) and separation factor of 1421, 4898 and 906 for dehydration of ethanol, ethyl acetate and dimethyl carbonate at 50 ºC, respectively.

Keywords: MXene, mixed matrix membrane, solvent dehydration, pervaporation, chitosan

1. Introduction

Dehydration of organic solvents such as alcohols and esters, is a key process in chemical industry, but energy intensive by using conventional separation methods. Alternatively, pervaporation technology provides an energy-saving and environmental-friendly approach for solvent dehydration[1]. Hydrophilic polymers like poly (vinyl alcohol) (PVA) and chitosan (CS), are the dominant membrane materials for pervaporation dehydration, while they generally suffer an undesirable trade-off between flux (permeability) and separation factor (selectivity) that limits their further application[2]. Several strategies have been proposed to improve the performance of polymeric membranes, among which mixed-matrix membrane (MMM) consisting of high-performing filler dispersed in polymer matrix has been considered as an effective approach[3, 4]. Apparently, one of the key for developing MMM is to choose the filler with high separation performance, as well as good compatibility with the polymer matrix. In the past decades, hydrophilic nanoparticles have been used as fillers to improve the dehydration performance of polymeric membranes. In particular, metal-organic framework (MOF) and MOF-derived nanomaterials with tunable pore size and organic linkers that possesses fast transport channels and high compatibility with polymer, has shown great potential in achieving higher flux and/or separation factor for alcohol dehydration and capacitor [5-11].

Recently, two-dimensional (2D) materials have been received great attention in membrane separation owing to the unique 2D transport channels by stacking the nanosheets[12-16]. Graphene oxide (GO), the derivative of graphene, exhibiting both 2D structure and hydrophilic property resulting from the oxygen-containing groups, have been incorporated into polymeric membranes for enhancing the pervaporation dehydration performance[17, 18]. Besides, other hydrophilic nanosheets also demonstrated capability in fabricating mixed-matrix pervaporation membranes with improved water transport properties[19]. As a new family of 2D materials, MXene[20-23], with a formula of $M_{n+1}X_nT_x$, where n is 1, 2, or 3, M stands for an early transition metal, X represents C and/or N, T refers to the surface group (OH, O, or F), has been employed for synthesizing separation membranes for wastewater treatment[24, 25], water desalination[26], ion sieving[27] and gas separation[16]. The resulting laminar structure and hydrophilicity of these MXene membranes endowed fast and selective transport of water molecules. Our previous work reported pristine MXene membranes with laminar structures for pervaporation desalination of NaCl solution[26]. However, to our best knowledge, the potential of MXene-based membranes for pervaporation dehydration of organic solvents has not been explored yet.

In this work, therefore, MXene ($Ti_3C_2T_x$) were incorporated into CS matrix to develop a new kind of mixed-matrix membranes for pervaporation dehydration of solvents. MXene nanosheets were synthesized by exfoliation followed by delamination of $Ti_3C_2T_x$ powders. The resulting MXene nanosheets dispersed in water were physically mixed with CS solution to form the MXene/CS MMMs. Morphologies, physicochemical properties and pervaporation performance of the resulting membranes were investigated with the introduction of MXene nanosheets. The solvent dehydration performance was tested in three typical azeotropic mixtures: water/ethanol, water/ethyl acetate or water /dimethyl carbonate mixtures. The effects of feed temperature and operation time on the pervaporation performance were studied as well.

2. Experimental

2.1 Materials

LiF (99.9%) was obtained from Aladdin Industrial Corporation, Shanghai China. HCl (36%-38%) was received from Lingfeng Chemical Reagent, China. Ethanol (>99.7%) was purchased from Yasheng Chemical Co. Ltd. CS (> 90% N-deacetylation degree) was obtained from Sinopharm Chemical Reagent Co., Ltd., China. The commercial polyacrylonitrile (PAN) ultrafiltration membrane was obtained from Shanghai Mega Vision Membrane Engineering & Technology Co. Ltd. Shanghai, China. Deionized water was used in the all experiments.

2.2 Synthesis of MXene nanosheets

The MXene nanosheets were synthesized at the aid of LiF and HCl, followed the method reported in our previous work[26]. In brief, 0.666 g Lithium fluoride was added into a plastic bottle (25 ml) with 10ml of a concentrated HCl solution (6M). After stirring for 40 min at room temperature, 1 g Ti_3AlC_2 powders were added particularly slowly into the above mixture. Then the mixed solution was reacting at 35℃ for one day under magnetically stirring. The resulting suspension was washed by large amount of ethanol until the pH reached about 6 and dried by vacuum drying. At last, the $Ti_3C_2T_x$ powders were obtained. A certain amount of $Ti_3C_2T_x$ powders were dispersed in DI water. In order to delaminate $Ti_3C_2T_x$ completely, powerful ultrasonication was introduced. The $Ti_3C_2T_x$ nanosheets would be gained after centrifugation for 1 h at 3500 r.p.m.

2.3 Fabrication of MXene/CS MMMs

Certain volume of MXene solution was diluted to 49 mL by DI water, then 1 mL acetic acid was added. After 2 h under stirring at room temperature, chitosan (CS,1.25 g) was dissolved in the above solution and remained for 18 h under stirring. To remove undissolved particles, the resultant solution was filtrated by gauze with pore size dozens of micrometer and then standing for few minutes to eliminate air bubbles. Commercial polyacrylonitrile (PAN) ultrafiltration membranes with very smooth surface and pore size of few tens of nanometers were used to support the MXene/CS MMMs and spin-coating was used to prepare membranes. The prepared membranes were dried at room temperature for 12 h and for further crosslinking reaction[28], the dried membranes were soaked in 2 mmol sulfuric acid solution for 24 h. Then, DI water was used to clean the membrane surface and dried at room temperature for another 12 h. For comparison, pure chitosan membrane was prepared by a similar approach. The MXene loading is calculated by the weight ratio of MXene over CS in the membrane.

2.4 Characterizations

The field emission scanning electron microscopy (Hitachi, S-4800, Japan) and Atomic Force Microscope (AFM, XE-100, Park SYSTEMS, Korea) were used to characterize the morphology of MXene nanosheets and composite membranes. Energy dispersive spectrometry (EDS) elemental mapping was taken using an energy dispersion of X-ray system equipped with a window connected to a FESEM S4800 operating at 30 kV. The membranes were characterized by Fourier transform infrared (FTIR, AVATAR-FT-IR-360, Thermo Nicolet, USA) spectra with the range of 500-3500 cm^{-1}). The X-ray photoelectron spectroscopy (XPS, Thermo ESCALAB 250, USA) characterization was carried out to check the groups of MXene/CS membranes. The water contact angle of MXene/CS membranes with different loading of MXene nanosheets were measured by the contact angle measurement system (DSA100, Kruss).

2.5 Pervaporation measurements

The pervaporation performance was measured with a home-made apparatus. The flat membrane was sealed in stainless steel made module. The feed solution circulated between membrane module and feed tank by a peristaltic pump with a speeding of 100 L/h to keep a turbulent flow. During the experiment process, the temperature on feed solution was maintained via thermostat water bath. The permeate pressure was below 200 Pa and we use a liquid nitrogen cold trap to collect the vapor on the permeate. The water content of feed and permeate side was detected by gas chromatography (GC2014, Japan). SE-34 capillary column was used and the analysis conditions are as follow: temperature for SPL1, Column and FID detector are 150, 90 and 150 °C, respectively. The injection mode is split with pressure of 35 kPa, total flow of 44.4 ml/min, column flow of 0.81ml/min and split ratio of 50.

The permeate flux and separation factor are usually used to evaluate membrane performance. The flux (J) and separation factor(α) can be calculated by the following equation:

$$J = \frac{M}{A \times t} \tag{1}$$

$$\alpha = \frac{y_w/(1-y_w)}{x_w/(1-x_w)} \tag{2}$$

where M (g) is the mass of permeate side collected by liquid nitrogen cold trap at a certain time t (h), A (m^2) represents the effective area of membrane. x_w and y_w are the water content in feed and permeate side, respectively.

3. Results and discussion

3.1 Morphology

MXene were produced successfully by removing the Al element from precursor Ti_3AlC_2 powders via HCl/LiF etching process, which was confirmed by the XRD patterns (Figure S1a). The nanosheets were obtained by exfoliating the MXene powders in water via sonication[29]. The BET specific surface area and pore volume was analyzed by N_2 adsorption-desorption of $Ti_3C_2T_x$ powder (Figure S1b). As shown in Figure 1, lateral size of the resulting MXene is 500-1000 nm, observed from AFM and SEM. The thickness of these MXene, measured by AFM, is 1-2 nm, indicating single- or double- layered MXene nanosheets were successfully synthesized[30]. These white spots might be due to the nanometer-sized impurity in the samples and the noise of AFM singal. The micron-meter lateral size whereas atomic-thin thickness features the 2D structure of MXene filler that is favorable for assembling 2D transport channels in the polymer matrix of mixed-matrix membranes. The physicochemical properties of the MXene nanosheets were further examined by XRD and XPS. The results agreed well with our previous work (Fig. S2 and S3), which are not shown here.

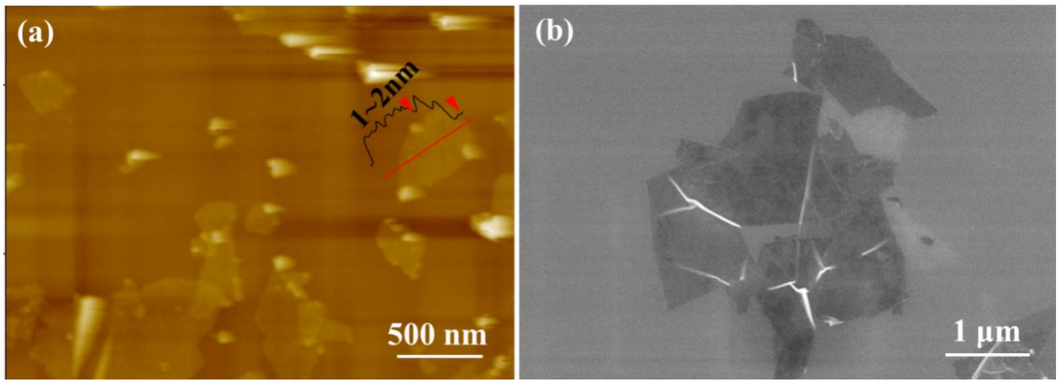

Figure 1. (a) AFM and (b) SEM images of synthesized MXene nanosheets for fabricating MMM.

To study the dispersion and interfacial morphology, dense films of CS MMM incorporated with MXene nanosheets were prepared. The cross-section SEM images of the film are shown in Figure S4a-c. Compared with the pristine CS membrane, MXene laminates can be observed in the MXene/CS MMMs.

The MXene is uniform dispersed in CS matrix with 3 wt% loading, while shows aggregation as the loading increases to 5 wt%. In either case, intact interfaces are achieved, suggesting a good compatibility between MXene and CS that is presumably owing to the molecular interactions between the hydroxyl groups of the filler and that of polymer chain. EDX was further performed to check the elemental distribution of the film cross-section (Figure S4d-e). In the pristine CS membrane, C and O elements were mainly detected, corresponding to the main chain of CS. In contrast, two more elements, Ti and Al, appeared in the CS MMM sample, confirming the incorporation of MXene. Specifically, the observed large amount of Ti single is attributed to a main element $Ti_3C_2T_x$ MXene, while the small Al peak results from the residual of etched Ti_3AlC_2 powder.

For practical application, asymmetric or composite MMM is required to obtain sufficient permeate flux and mechanical strength, as well as to reduce the membrane cost. Thus, the MXene/CS mixed-matrix solution was coated on a porous PAN substrate via spinning technique. As shown in Figure 2, sub-micron thick mixed-matrix separation layer was achieved, with an average membrane thickness of ~500 nm for both pristine CS and MXene incorporated CS MMMs. The membrane surface looks dense without any visible defects, and the active layer was firmly deposited on top of the PAN substrate. This thin composite membrane structure is critical for decreasing the transport resistance and thus increasing the permeate flux of the MMMs[3]. It’s noted that it’s not easy to clearly see the MXene laminates in the thin mixed-matrix layer as the MXene loading in the matrix is no more than 3 wt% (Figure 2f, g). While a laminate-like structure was observed in the 5 wt% MXene/CS layer (Figure 2h), which is due to the aggregation of MXene nanosheets in the CS according to the SEM result of dense film (Figure S3c).

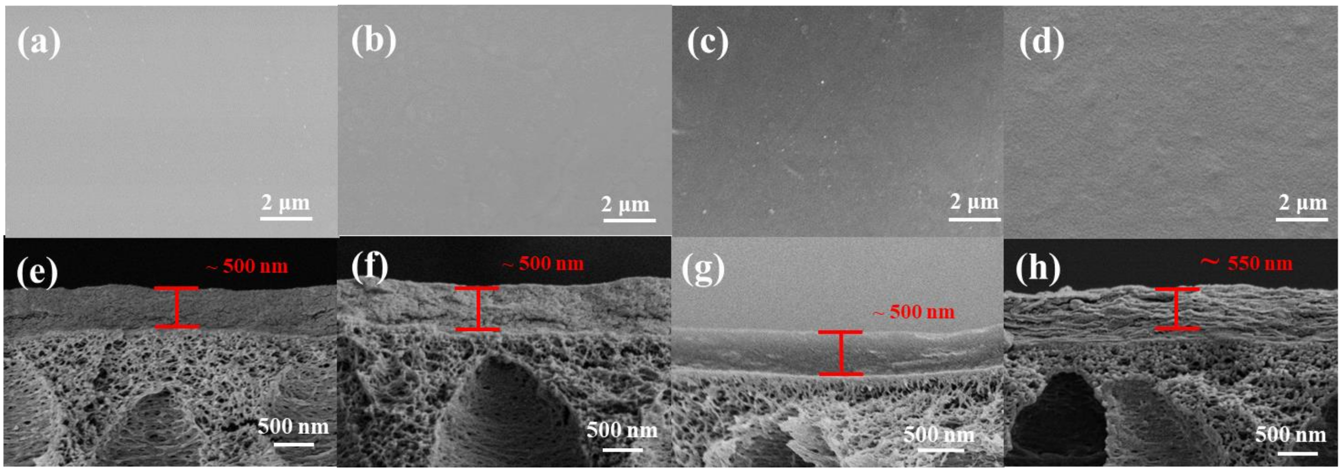

Figure 2. SEM images of MXene/CS mixed-matrix composite membranes prepared on porous PAN substrate with different MXene loading (a, e) 0%, (b, f) 1%, (c, g) 3%,(d, h) 5%. (a-d) membrane surface; (e-h) membrane cross-section.

Moreover, AFM was used to probe the fine nanostructure of membrane surface. As shown in Figure 3, the morphology of 3 wt% MXene/CS MMM is as homogenous as the pristine CS membrane, while some large domains can be found in the 5 wt% MXene/CS MMM. Combined with the SEM results, these domains can be attributed to the aggregation of MXene nanosheets in the CS membrane.

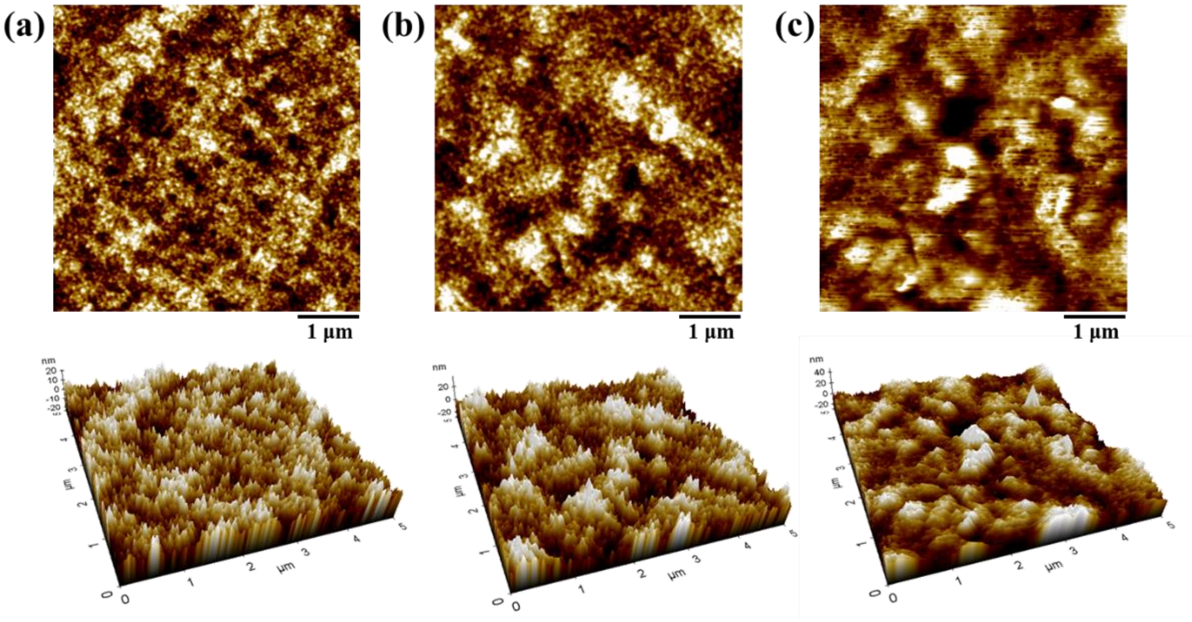

Figure 3. AFM images of MXene/CS MMMs with different MXene loading: (a) 0 wt%; (b) 3 wt%; (c) 5 wt%.

3.2 Chemical property

The chemical property of the CS membrane before and after incorporating MXene nanosheets was analyzed by FTIR. As shown in Figure 4a, the absorption bands at 3360, 1633 and 1527 cm^{-1} are corresponding to –OH, –C=O and $–NH_2$ groups of CS, respectively[31]. The IR spectrum of MXene also exhibited two peaks at 3360 and 1633 cm^{-1}[24], which overlap with that of CS. XPS was further employed to analyze the chemical structure of CS membrane and MXene/CS MMM. Figure 4b-c present the C1s spectra, suggesting the peaks around 284.8, 286.3, 287.8 eV, corresponding to the –C–C, –C–N and –O–C–O groups, respectively[32]. From the XPS result, the C1S composition in the CS membrane and 3 wt% MXene/CS membrane are 65.73% and 62.94%, respectively.

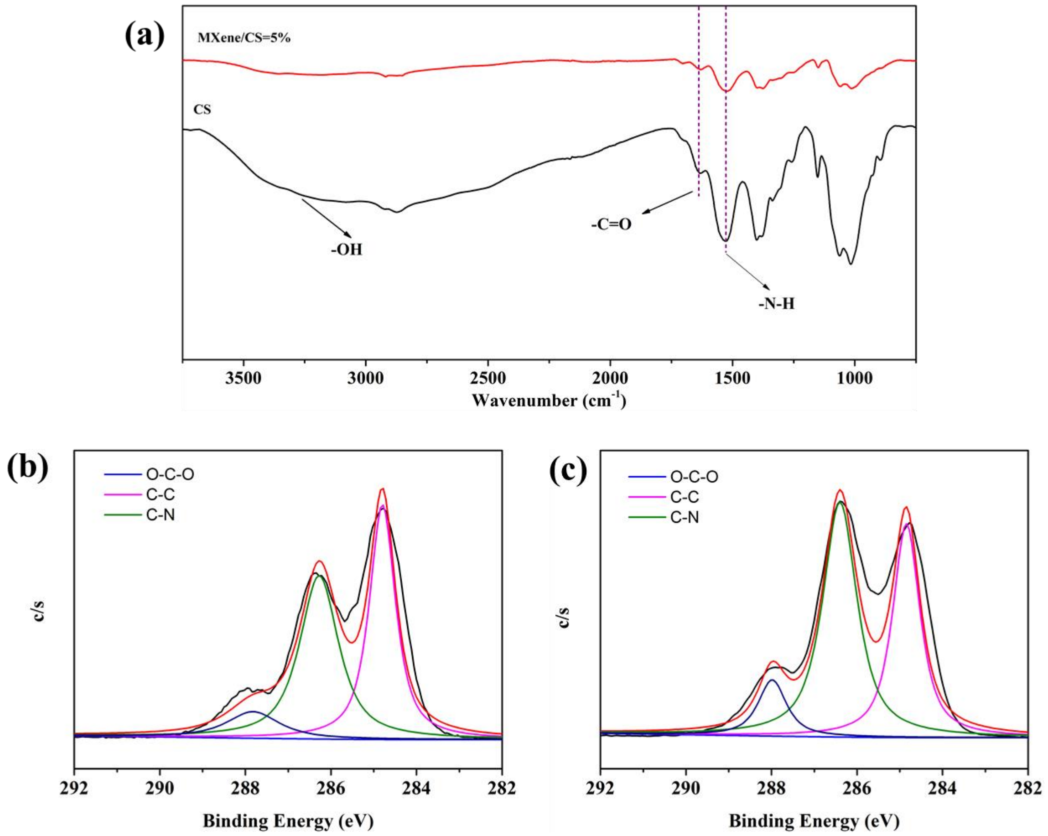

Figure 4. (a) FTIR spectra of CS and 5 wt% MXene/CS membranes; XPS C1s scan of (b) CS and (c) 3 wt% MXene/CS membranes.

3.3 Surface hydrophilicity

Surface hydrophilicity is a key characteristic for pervaporation membrane since it mainly determines the sorption behavior of feed liquids on the membrane surface[33]. Here, water contact angle was used to evaluate the surface hydrophilicity of MXene/CS MMMs with various MXene loading. As shown in Figure S5, the water contact angle on the membrane surface was not significantly varied by incorporating the MXene nanosheets. It's speculated that the hydrophilicity of MXene is as high as that of CS, thereby remaining the surface hydrophilicity of MXene/CS at various MXene loading.

3.4 Separation performance

The pervaporation performance of the MXene/CS mixed-matrix composite membranes prepared on PAN substrate (Figure 2) was firstly evaluated by dehydration of water/ethanol mixtures that is a key component for biofuel production[34, 35]. The effect of MXene loading on the pervaporation dehydration performance was studied. As shown in Figure 5, a simultaneous increase in total flux and separation factor of CS membrane is achieved by introducing the MXene nanosheets with loading up to 3 wt%. The total flux and separation factor of the pristine CS membrane was highly improved from ~1.1 to 1.4 kg/(m^2 h), and from 407 to 1421, respectively. According to the solution-diffusion model[36], both sorption and diffusion contribute to the pervaporation permeation process. The water contact angle test indicated a nearly unchanged surface hydrophilicity of the membrane with incorporating hydrophilic MXene nanosheets into the hydrophilic CS matrix. It may lead a similar water sorption behavior either in pristine CS or MXene/CS MMMs. Thus, the remarkable improvement in flux and separation factor can be attributed to the enhanced selective diffusion of water molecules over ethanol[17, 19]. It's presumably that in the CS matrix the MXene nanosheets were assembled into laminates whose interlayer channels promote the water transport[26]. It's also noticed that the dehydration performance was declined as increasing the MXene loading to 5 wt%, which could be due to the non-selective defects formed by the aggregation of MXene at excessive high loading as indicated by Figure S3c and Figure 2h. Here, 3 wt% was considered as the optimal loading for fabricating MXene/CS MMM.

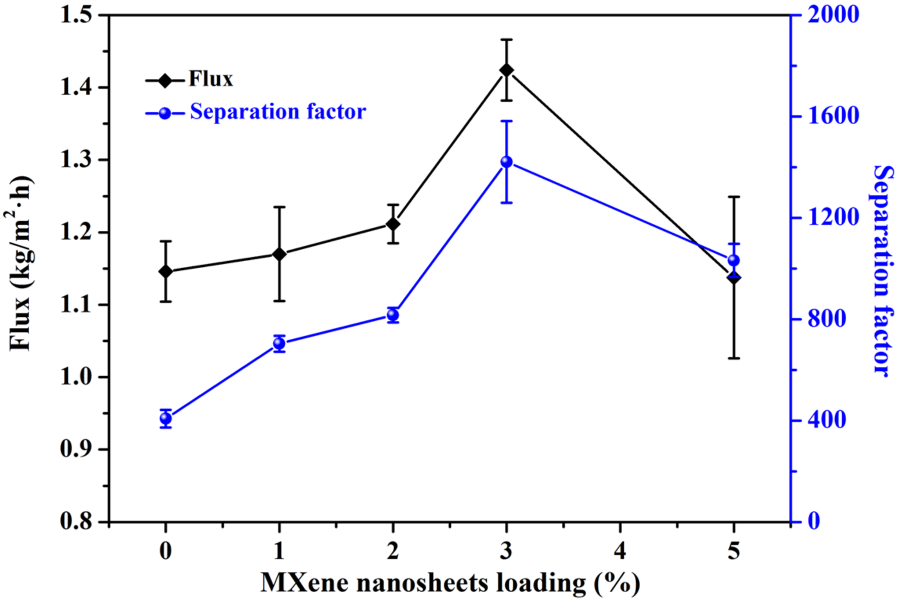

Figure 5. Effect of MXene loading on the pervaporation performance of MXene/CS MMMs for dehydration of 90 wt% water /ethanol mixtures at 50 °C. The error bars are generated by averaging the data from three different membrane samples.

Besides of ethanol, the dehydration of other typical solvents, ethyl acetate and dimethyl carbonate, which are widely used in industry and would also form azeotropy with water, was investigated by using the above-optimized MXene/CS MMM with 3 wt% MXene loading. Water content was fixed at 2 wt% based on the solubility and azeotrope of the ethyl acetate[37] or dimethyl carbonate[38] mixed with water. The pervaporation results are given in Figure 6. As expected, both total flux and separation factor of MXene/CS MMM are higher than that of pristine CS membrane for dehydration of ethyl acetate or dimethyl carbonate. Moreover, compared with ethanol, the separation factor for ethyl acetate is much higher while for dimethyl carbonate is slightly lower, which might be caused by the variable molecular interactions between water and the solvent[37]. Regardless, the MXene-induced higher total flux and water/solvent separation factor show a nice consistency with those observed in ethanol dehydration process (Figure 5). It suggests that the proposed water-transport channels within the MXene laminates embedded in CS matrix are not only highly efficient for dehydration of ethanol, but also for other solvents with different molecular size and chemical groups, for instance the ethyl acetate and dimethyl carbonate demonstrated here. The application of this MXene/CS MMM for dehydration of different kinds of solvents (e.g., propanol, butanol) is under progress.

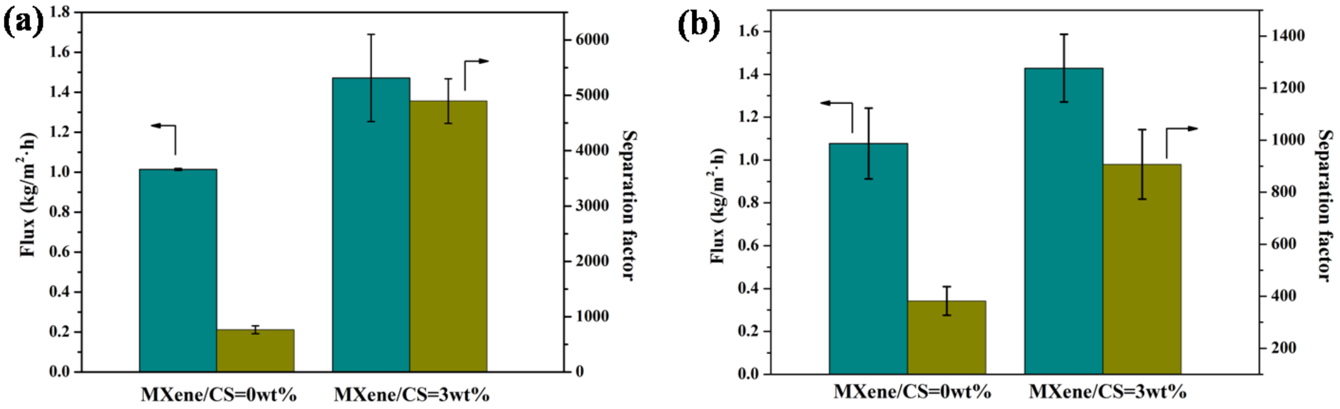

Figure 6. Pervaporation performance of 3 wt% MXene/CS MMM for dehydration of (a) 98 wt% water /ethyl acetate mixtures and (b) 98 wt% water / dimethyl carbonate mixtures at 50 °C. The error bars are generated by averaging the data from three different membrane samples.

Effect of operating temperature on the dehydration performance of MXene/CS MMM was studied in the water / ethyl acetate mixtures. As displayed in Figure 7a, the flux is increased whereas the separation factor is decreased with increasing the feed temperature, which agrees well with the general phenomena in polymer-based pervaporation membranes[2]. Higher temperature creates higher driving force for the molecular diffusion, as well as more swelling of the polymer matrix, both of which can lead higher permeate flux. While the swelling of polymer matrix would decline the size discrimination effect of free-volume cavities within the membrane, thereby resulting in the lower separation factor at higher temperature. With the individual flux at various temperature, Arrhenius plots (Figure 7b) can be made to study the activation energy of water and ethyl acetate permeating through the MXene/CS MMM by using the Arrhenius equation[39]:

(3)

where the J_i is the permeate flux of component i (kg m^{-2} h^{-1}), A_i is the preexponential factor (kg m^{-2} h^{-1}), Ea is the activation energy (kJ mol^{-1}), R is the gas constant (kJ mol^{-1} K^{-1}) and T is the feed temperature (K). The calculated activation energy of water and ethyl acetate are 9.64 and 31.2 kJ/mol, respectively (goodness of the fitting for calculating Ea of water and ethyl acetate is 0.94 and 0.89, respectively). The much higher ethyl acetate activation energy indicates the higher temperature sensitivity of ethyl acetate permeation over water permeation.

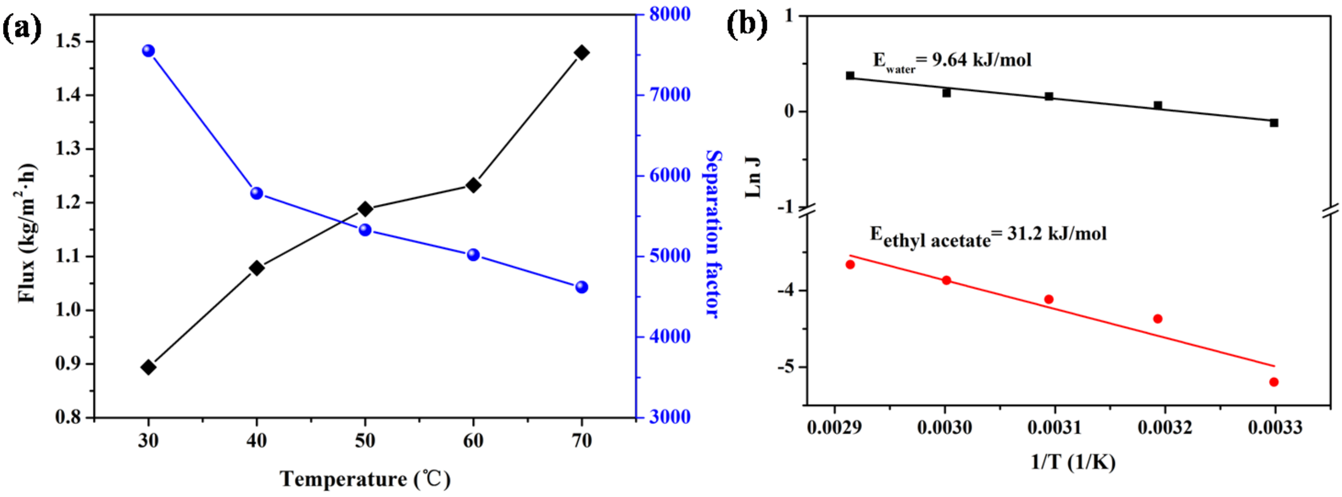

Figure 7. Effect of operating temperature on pervaporation performance of 3 wt% MXene/CS MMM for dehydration of 98 wt% water /ethyl acetate mixtures: (a) flux and separation factor; (b) Arrhenius plots for water and ethyl acetate flux.

Long-term stability is another important factor for the pervaporation dehydration. Thus, the influence of operating time on the dehydration performance of MXene/CS MMM was studied as well. As shown in Figure 8, the flux and water content in permeate are stable during the continuous dehydration of water /ethyl acetate mixtures for ~1800 min. The observed slight fluctuations of dehydration performance are due to the variation of feed concentration. This result indicates a good structural stability of the MXene/CS MMM under cross-flow turbulence with a feed rate of 100 L/h and temperature of 50 °C.

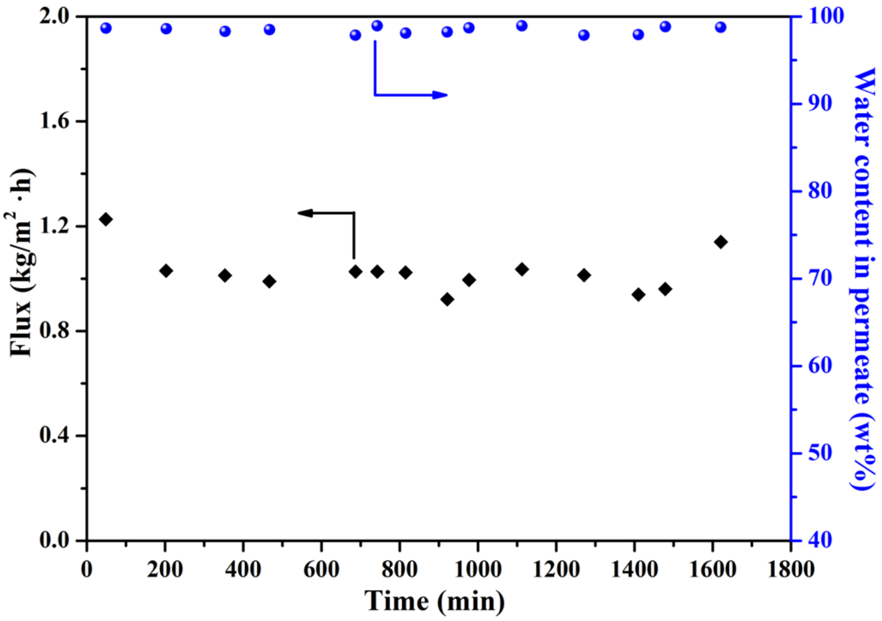

Figure 8. Effect of operating time on pervaporation performance of 3 wt% MXene/CS MMM for dehydration of 98 wt% water /ethyl acetate mixtures at 50 °C.

Table 1 lists the solvent dehydration performance of MXene/CS MMM compared with reported membranes. In all the tested solvent/water mixtures, the prepared MXene/CS MMM exhibited higher total flux and/or separation factor than the most polymer-based membranes. The performance of MXene-incorporated CS membrane, although with only 3 wt% loading, is also comparable to that of another 2D materials, GO membranes with laminar structures[40, 41]. Compared to MOF and GO, due to the existence of abound oxygen-containing groups, the MXene nanosheets showed a good hydrophilicity, which can facilitate water molecular preferential adsorption on the MXene/CS MMM surface. Besides, MXene nanosheets can provide 2D pathway to achieve rapid mass transfer. It can be expected that, laminar MXene membrane, once successfully prepared, would show much higher performance for solvent dehydration.

Table 1. Pervaporation performance of MXene/CS MMM compared with reported membranes for solvent dehydration.

Membrane	Feed temperature (K)	Feed water concentration (wt%)	Total flux (g m^{-2} h^{-1})	Separation factor	Ref
Wate/ethyl acetate mixtures					
Perfluorosulfonic acid-TEOS	313	2.0	205	496	[42]
PBI/PEI	333	2.0	820	2478	[43]
CS	313	2.0	336	6270	[44]

PVA	313	2.0	35	7270	[45]
PVA	323	2.0	22	5000	[46]
UiO-66@graphene oxide	323	2.0	3233	6951	[41]
MXene/CS	323	2.0	1471	4898	This work
Water/ethanol mixtures					
POSS/CS	333	10	270	30	[47]
Graphene/CS	303	10	10	1093	[48]
Fe_3O_4/CS	350	10	1024	1500	[49]
MOF-801/CS	343	10	1937	2156	[41]
MXene/CS	323	10	1424	1421	This work
Water/dimethyl carbonate mixtures					
CS	298	2.6	49	337	[38]
PVA	323-343	2.7	800	644	[50]
Graphene oxide	313	2.0	1400	484	[40]
MXene/CS	323	2.0	1428	906	This work

4. Conclusions

In this work, MXene nanosheets were synthesized and used as 2D filler to improve the solvent dehydration performance of CS membrane via mixed-matrix approach. Submicron-thick MXene/CS mixed-matrix composite membranes were fabricated on porous PAN substrate via spin-coating. The incorporated MXene laminates with interlayer channels endow a fast and selective transport of water molecules, thereby highly enhancing the flux and meanwhile separation factor of pristine CS membrane for solvent dehydration. The resulting MXene/CS MMM with optimized MXene loading of 3 wt% exhibited flux of ~1.4-1.5 kg/(m^2 h) and separation factor of 1421, 4898 and 906 for dehydration of ethanol, ethyl acetate and dimethyl carbonate at 50 ºC. This performance is higher than that of state-of-the-art membranes, demonstrating the great potential of MXene-based membranes for solvent dehydration.

Acknowledgements

Dr. Xu is sponsored by China Regenerative Medicine International (CRMI) through a technology centre grant. This work is financially supported by the National Natural Science Foundation of China (Grant Nos. 21490585, 21476107, 51861135203), the Innovative Research Team Program by the Ministry of Education of China (Grant No. IRT17R54).

References

[1] P.D. Chapman, T. Oliveira, A.G. Livingston, K. Li, Membranes for the dehydration of solvents by pervaporation, Journal of Membrane Science, 318 (2008) 5-37.

[2] Y.K. Ong, G.M. Shi, N.L. Le, Y.P. Tang, J. Zuo, S.P. Nunes, T.-S. Chung, Recent membrane development for pervaporation processes, Progress in Polymer Science, 57 (2016) 1-31.

[3] X. Cheng, F. Pan, M. Wang, W. Li, Y. Song, G. Liu, H. Yang, B. Gao, H. Wu, Z. Jiang, Hybrid membranes for pervaporation separations, Journal of Membrane Science, 541 (2017) 329-346.

[4] P.-Y. Hsu, T.-Y. Hu, S.R. Kumar, C.-H. Chang, K.C.W. Wu, K.-L. Tung, S.J. Lue, Highly Zeolite-Loaded Polyvinyl Alcohol Composite Membranes for Alkaline Fuel-Cell Electrolytes, Polymers, 10 (2018).

[5] X. Cheng, Z. Jiang, X. Cheng, S. Guo, L. Tang, H. Yang, H. Wu, F. Pan, P. Zhang, X. Cao, B. Wang, Bimetallic metal-organic frameworks nanocages as multi-functional fillers for water-selective membranes, Journal of Membrane Science, 545 (2018) 19-28.

[6] G. Liu, Z. Jiang, K. Cao, S. Nair, X. Cheng, J. Zhao, H. Gomaa, H. Wu, F. Pan, Pervaporation performance comparison of hybrid membranes filled with two-dimensional ZIF-L nanosheets and zero-dimensional ZIF-8 nanoparticles, Journal of Membrane Science, 523 (2017) 185-196.

[7] G.M. Shi, T. Yang, T.S. Chung, Polybenzimidazole (PBI)/zeolitic imidazolate frameworks (ZIF-8) mixed matrix membranes for pervaporation dehydration of alcohols, Journal of Membrane Science, 415-416 (2012) 577-586.

[8] M. Vinu, D.S. Raja, Y.-C. Jiang, T.-Y. Liu, Y.-Y. Xie, Y.-F. Lin, C.-C. Yang, C.-H. Lin, S.M. Alshehri, T. Ahamad, R.R. Salunkhe, Y. Yamauchi, Y.-H. Deng, K.C.W. Wu, Effects of structural crystallinity and defects in microporous Al-MOF filled chitosan mixed matrix membranes for pervaporation of water/ethanol mixtures, Journal of the Taiwan Institute of Chemical Engineers, 83 (2018) 143-151.

[9] Y.V. Kaneti, S. Dutta, M.S.A. Hossain, M.J.A. Shiddiky, K.-L. Tung, F.-K. Shieh, C.-K. Tsung, K.C.W. Wu, Y. Yamauchi, Strategies for Improving the Functionality of Zeolitic Imidazolate Frameworks: Tailoring Nanoarchitectures for Functional Applications, Advanced Materials, 29 (2017).

[10] Y.V. Kaneti, J. Tang, R.R. Salunkhe, X. Jiang, A. Yu, K.C.W. Wu, Y. Yamauchi, Nanoarchitectured Design of Porous Materials and Nanocomposites from Metal-Organic Frameworks, Advanced Materials, 29 (2017).

[11] F.-K. Shieh, S.-C. Wang, C.-I. Yen, C.-C. Wu, S. Dutta, L.-Y. Chou, J.V. Morabito, P. Hu, M.-H. Hsu, K.C.W. Wu, C.-K. Tsung, Imparting Functionality to Biocatalysts via Embedding Enzymes into Nanoporous Materials by a de Novo Approach: Size-Selective Sheltering of Catalase in Metal-Organic Framework Microcrystals, Journal of the American Chemical Society, 137 (2015) 4276-4279.

[12] G. Liu, W. Jin, N. Xu, Two-Dimensional-Material Membranes: A New Family of High-Performance Separation Membranes, Angewandte Chemie International Edition, 55 (2016) 13384-13397.

[13] G. Liu, W. Jin, N. Xu, Graphene-based membranes, Chemical Society Reviews, 44 (2015) 5016-5030.

[14] X. Zhu, C. Tian, D.-T. Chi-Linh, S. Dai, Two-Dimensional Materials as Prospective Scaffolds for Mixed-Matrix Membrane-Based CO2 Separation, Chemsuschem, 10 (2017) 3304-3316.

[15] V. Veeramani, M. Sivakumar, S.M. Chen, R. Madhu, H.R. Alamri, Z.A. Alothman, M.S.A. Hossain, C.K. Chen, Y. Yamauchi, N. Miyamoto, Lignocellulosic biomass-derived, graphene sheet-like porous activated carbon for electrochemical supercapacitor and catechin sensing, Rsc Advances, 7 (2017).

[16] J. Wang, Y. Xu, B. Ding, Z. Chang, X. Zhang, Y. Yamauchi, K.C.W. Wu, Confined Self-Assembly in Two-Dimensional Interlayer Space: Monolayered Mesoporous Carbon Nanosheets with In-Plane Orderly Arranged Mesopores and a Highly Graphitized Framework, Angewandte Chemie-International Edition, 57 (2018) 2894-2898.

[17] K. Cao, Z. Jiang, J. Zhao, C. Zhao, C. Gao, F. Pan, B. Wang, X. Cao, J. Yang, Enhanced water permeation through sodium alginate membranes by incorporating graphene oxides, Journal of Membrane Science, 469 (2014) 272-283.

[18] J. Zhao, Y. Zhu, G. He, R. Xing, F. Pan, Z. Jiang, P. Zhang, X. Cao, B. Wang, Incorporating Zwitterionic Graphene Oxides into Sodium Alginate Membrane for Efficient Water/Alcohol Separation, ACS Applied Materials & Interfaces, 8 (2016) 2097-2103.

[19] K. Cao, Z. Jiang, X. Zhang, Y. Zhang, J. Zhao, R. Xing, S. Yang, C. Gao, F. Pan, Highly water-selective hybrid membrane by incorporating g-C3N4 nanosheets into polymer matrix, Journal of Membrane Science, 490 (2015) 72-83.

[20] M. Naguib, M. Kurtoglu, V. Presser, J. Lu, J. Niu, M. Heon, L. Hultman, Y. Gogotsi, M.W. Barsoum, Two-Dimensional Nanocrystals Produced by Exfoliation of Ti3AlC2, Advanced Materials, 23 (2011) 4248-4253.

[21] O. Mashtalir, M. Naguib, V.N. Mochalin, Y. Dall'Agnese, H. Min, M.W. Barsoum, Y. Gogotsi, Intercalation and delamination of layered carbides and carbonitrides, Nature Communications, 4 (2013) 1716.

[22] K. Maleski, V.N. Mochalin, Y. Gogotsi, Dispersions of Two-Dimensional Titanium Carbide MXene in Organic Solvents, Chemistry of Materials, 29 (2017).

[23] X. Xie, M.Q. Zhao, B. Anasori, K. Maleski, C.E. Ren, J. Li, B.W. Byles, E. Pomerantseva, G. Wang, Y. Gogotsi, Porous heterostructured MXene/carbon nanotube composite paper with high volumetric capacity for sodium-based energy storage devices, Nano Energy, 26 (2016) 513-523.

[24] L. Ding, Y. Wei, Y. Wang, H. Chen, J. Caro, H. Wang, A Two-Dimensional Lamellar Membrane: MXene Nanosheet Stacks, Angewandte Chemie International Edition, 56 (2017) 1825-1829.

[25] R. Han, X. Ma, Y. Xie, D. Teng, S. Zhang, Preparation of a new 2D MXene/PES composite membrane with excellent hydrophilicity and high flux, Rsc Advances, 7 (2017) 56204-56210.

[26] G. Liu, J. Shen, Q. Liu, G. Liu, J. Xiong, J. Yang, W. Jin, Ultrathin two-dimensional MXene membrane for pervaporation desalination, Journal of Membrane Science, 548 (2018) 548-558.

[27] C.E. Ren, K.B. Hatzell, M. Alhabeb, Z. Ling, K.A. Mahmoud, Y. Gogotsi, Charge- and Size-Selective Ion Sieving Through Ti3C2Tx MXene Membranes, The Journal of Physical Chemistry Letters, 6 (2015) 4026-4031.

[28] A. Kamari, W.S.W. Ngah, M.Y. Chong, M.L. Cheah, Sorption of acid dyes onto GLA and H_2SO_4 cross-linked chitosan beads, Desalination, 249 (2009) 1180-1189.

[29] M. Ghidiu, M.R. Lukatskaya, M.-Q. Zhao, Y. Gogotsi, M.W. Barsoum, Conductive two-dimensional titanium carbide ‘clay’ with high volumetric capacitance, Nature, 516 (2014) 78.

[30] A. Lipatov, M. Alhabeb, M.R. Lukatskaya, A. Boson, Y. Gogotsi, A. Sinitskii, Effect of Synthesis on Quality, Electronic Properties and Environmental Stability of Individual Monolayer Ti3C2 MXene Flakes, Advanced Electronic Materials, 2 (2016) 1600255-n/a.

[31] Y. Zhu, S. Xia, G. Liu, W. Jin, Preparation of ceramic-supported poly(vinyl alcohol)–chitosan composite membranes and their applications in pervaporation dehydration of organic/water mixtures, Journal of Membrane Science, 349 (2010) 341-348.

[32] F.C. de Godoi, E. Rodriguez-Castellon, E. Guibal, M.M. Beppu, An XPS study of chromate and vanadate sorption mechanism by chitosan membrane containing copper nanoparticles, Chemical Engineering Journal, 234 (2013) 423-429.

[33] G. Liu, F. Xiangli, W. Wei, S. Liu, W. Jin, Improved performance of PDMS/ceramic composite pervaporation membranes by ZSM-5 homogeneously dispersed in PDMS via a surface graft/coating approach, Chemical Engineering Journal, 174 (2011) 495-503.

[34] B. Bolto, M. Hoang, Z. Xie, A review of membrane selection for the dehydration of aqueous ethanol by pervaporation, Chemical Engineering and Processing: Process Intensification, 50 (2011) 227-235.

[35] L.M. Vane, Separation technologies for the recovery and dehydration of alcohols from fermentation broths, Biofuels, Bioproducts and Biorefining, 2 (2008) 553-588.

[36] J.G. Wijmans, R.W. Baker, The solution-diffusion model: a review, Journal of Membrane Science, 107 (1995) 1-21.

[37] S. Xia, X. Dong, Y. Zhu, W. Wei, F. Xiangli, W. Jin, Dehydration of ethyl acetate–water mixtures using PVA/ceramic composite pervaporation membrane, Separation and Purification Technology, 77 (2011) 53-59.

[38] W. Won, X. Feng, D. Lawless, Separation of dimethyl carbonate/methanol/water mixtures by pervaporation using crosslinked chitosan membranes, Separation and Purification Technology, 31 (2003) 129-140.

[39] X. Feng, R.Y. Huang, Estimation of activation energy for permeation in pervaporation processes, Journal of Membrane Science, 118 (1996) 127-131.

[40] K. Huang, G. Liu, Y. Lou, Z. Dong, J. Shen, W. Jin, A Graphene Oxide Membrane with Highly Selective Molecular Separation of Aqueous Organic Solution, Angewandte Chemie International Edition, 53 (2014) 6929-6932.

[41] Y. Ying, D. Liu, W. Zhang, J. Ma, H. Huang, Q. Yang, C. Zhong, High-Flux Graphene Oxide Membranes Intercalated by Metal–Organic Framework with Highly Selective Separation of Aqueous Organic Solution, ACS Applied Materials & Interfaces, 9 (2017) 1710-1718.

[42] H.-K. Yuan, Z.-L. Xu, J.-H. Shi, X.-H. Ma, Perfluorosulfonic acid—Tetraethoxysilane/polyacrylonitrile (PFSA-TEOS/PAN) hollow fiber composite membranes prepared for pervaporation dehydration of ethyl acetate–water solutions, Journal of Applied Polymer Science, 109 (2008) 4025-4035.

[43] Y. Wang, Pervaporation Dehydration of Ethyl Acetate via PBI/PEI Hollow Fiber Membranes, Industrial & Engineering Chemistry Research, 54 (2015) 3082-3089.

[44] X.-H. Ma, Z.-L. Xu, C.-Q. Ji, Y.-M. Wei, H. Yang, Characterization, separation performance, and model analysis of STPP-chitosan/PAN polyelectrolyte complex membranes, Journal of Applied Polymer Science, 120 (2011) 1017-1026.

[45] H.-K. Yuan, J. Ren, X.-H. Ma, Z.-L. Xu, Dehydration of ethyl acetate aqueous solution by pervaporation using PVA/PAN hollow fiber composite membrane, Desalination, 280 (2011) 252-258.

[46] Y. Salt, A. Hasanoğlu, İ. Salt, S. Keleşer, S. Özkan, S. Dinçer, Pervaporation separation of ethylacetate–water mixtures through a crosslinked poly(vinylalcohol) membrane, Vacuum, 79 (2005) 215-220.

[47] D. Xu, L.S. Loo, K. Wang, Pervaporation performance of novel chitosan-POSS hybrid membranes: Effects of POSS and operating conditions, Journal of Polymer Science Part B: Polymer Physics, 48 (2010) 2185-2192.

[48] D.P. Suhas, T.M. Aminabhavi, H.M. Jeong, A.V. Raghu, Hydrogen peroxide treated graphene as an effective nanosheet filler for separation application, RSC Advances, 5 (2015) 100984-100995.

[49] R. Xing, H. Wu, C. Zhao, H. Gomaa, J. Zhao, F. Pan, Z. Jiang, Fabrication of Chitosan Membranes with High Flux by Magnetic Alignment of In Situ Generated Fe3O4, Chemical Engineering & Technology, 39 (2016) 969-978.

[50] A. Nickel, W. Arlt, I. Janisch, P. Wagner, A. Klausener, Process for separating off alkanols, mixtures of alkanols and water or water itself from oxygen-containing organic compounds of higher carbon number, in, US 5360923 A, 1994.